

Compatibility Effects of Waste Cooking Oil Biodiesel Blend on Fuel System Elastomers in Compression Ignition Engines

Elumalai Perumal Venkatesan,* Ravi Krishnaiah,* Kalapala Prasad, Sreenivasa Reddy Medapati, Sripada Rama Sree, Mohammad Asif, Sher Afghan Khan, and Emanoil Linul*



Cite This: *ACS Omega* 2024, 9, 6709–6718



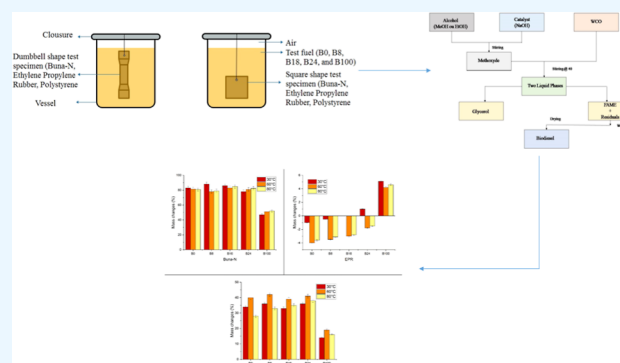
Read Online

ACCESS |

Metrics & More

Article Recommendations

ABSTRACT: Alternative energy sources, such as biodiesel, play a vital role in environmental protection. Waste cooking oil (WCO) biodiesel has promising applications in compression ignition engines. A major problem regarding biodiesel implementation is the deterioration and materials incompatibility of existing fuel system components with biodiesel. Variations in the composition of fuel prompted by the inclusion of biodiesel cause a variety of issues in diesel engine fuel systems where the elastomer is generally utilized as the fuel hose material and sealings. In this experimental work, the effects of the diesel and WCO biodiesel blends (B8, B16, B24, and B100) on Buna-N, ethylene propylene rubber (EPR), and polystyrene (PS) were examined by the immersion test, which was conducted for 160 h at various immersion temperatures of 30, 60, and 80 °C, respectively. The study also showed that the use of elastomer materials like Buna-N, EPR, and PS in diesel engines fueled up to 20% WCO biodiesel blends is advantageous; the overall compatibility improves by 100% compared to that obtained using neat diesel. The outcome revealed remarkable behavior changes, including a minor increase in volume and a slight loss in tensile strength and hardness compared to that observed using neat diesel fuel. The expansion of rubber materials increases over 60 °C, although the rate of this process decreases above 80 °C. It has been found that the expansion of rubber materials is unaffected by the acid concentration of the WCO biodiesel blends but significantly affected by the moisture content.



INTRODUCTION

Crude oil is heavily relied on by the transportation sector in China. Its dependence on foreign crude oil increased to roughly 74.5% by 2020.^{1–3} However, China is largely restructuring its energy consumption and reducing its dependence on crude oil, thanks to the use of sustainable biofuels in the transportation sector, such as ethanol and biodiesel.^{4–6} The rest of the world is also emphasizing the use of renewable energy sources, particularly biofuels such as ethanol and biodiesel. Additionally, the European Union (EU), Brazil, the United States (US), and a few Southeast Asian nations use biodiesel widely as the most effective and environmentally beneficial fuel.⁷ In a similar vein, agrofuel is expanding in markets in the US, EU, Brazil, and Southeast Asian nations. Additionally, by 2021, the US, Brazil, and EU had set targets of 15, 30, and 35% of agrofuel blends over all gasoline usage, respectively.⁸ The typical agrofuel raw materials include soybean oil, rapeseed oil, palm oil, other edible oils, jatropha, castor, and other nonedible oils, as well as a few sustainable resources such as waste cooking oil (WCO) and animal fats.⁹ A facility was created specifically for the study on biodiesel manufacture, which will produce 39,208 t of biodiesel

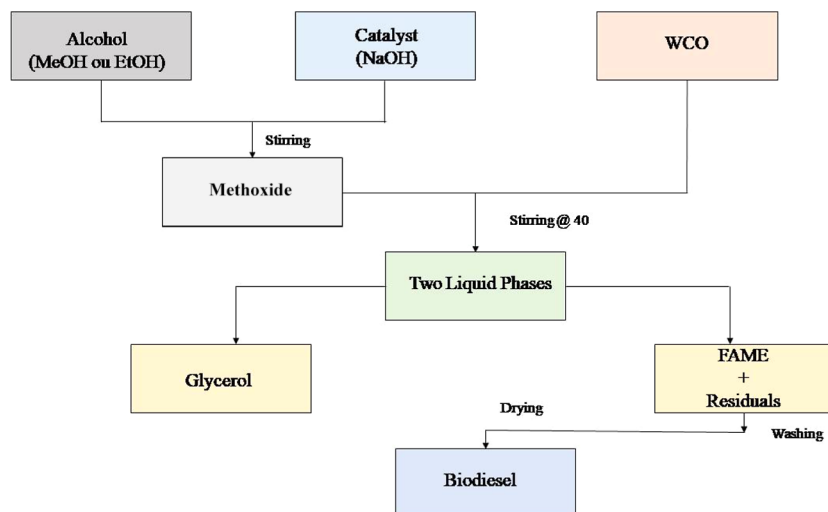
yearly. The estimated total capital cost for this development is Rs. 1,615,122,000. Using a price of Rs. 12/kg for the feedstock, WCO, a cost of Rs. 50/kg for biodiesel was computed.¹⁰ China consumed 33 million tonnes of edible oil in 2019, of which 11.5 million tonnes were primarily imported from foreign nations. The focus of China Town has switched to being a possible source of (20–30%) biodiesel raw materials due to the lack of edible oil in biodiesel manufacturing; WCO is mostly supplied by cities with dense populations, including Shenzhen, Tianjin, Shanghai, and Zhengzhou. Different feedstocks were produced by altering the components of Fatty Acid Methyl Esters (FAMES). The WCO genres employed in the production process significantly impact the ingredients used in the WCO biodiesel. Furthermore, there is relatively little knowledge regarding WCO agrofuels' compat-

Received: October 9, 2023
Revised: November 23, 2023
Accepted: November 28, 2023
Published: February 1, 2024

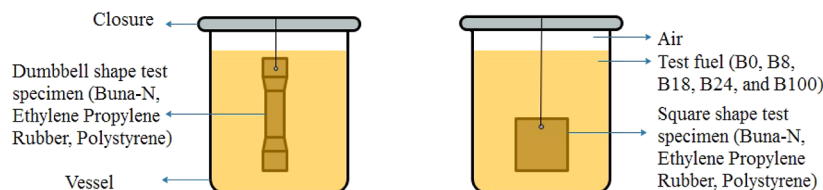


Table 1. Literature on Details of WCO Biodiesel Compared with Diesel

| reference | engine particular | performance parameter | | emission parameter | |
|-----------|--|-----------------------|------------|-------------------------------------|-------------------------------------|
| | | increased | decreased | increased | decreased |
| 27 | 1C, 4S, DI, IP 230 bar, 1500 rpm, IT 24 bTDC | 0.44 kg/kW h BSFC | 26.1% BTE | 39.21% EGT 48.4% NO _x | 44.05% CO 36.22% HC 18.63% smoke |
| 28 | 1C, 4S, DI, 4.4 kW, 1500 rpm | BSFC | 27.2% BTE | 18.32% NO _x | 54.17% CO 50% HC 22.69% smoke |
| 29 | 1C, 4S, DI, 12 N m, 2400 rpm | 7.51% BTE | 8.89% BSFC | 4.64% NO _x | 7.69% CO |
| 30 | 1C, 4S, DI, 5.75 kW, 1500 rpm, IT 24 bTDC | 28.3% BSFC | 29% BTE | 33% HC 11% smoke | 45% CO 65% NO _x |
| 31 | 1C, 4S, DI, 3.5 kW, 1500 rpm, IT 23 bTDC | 1.22% BTE | BSFC | | 4.07% NO _x 29.38% smoke |

**Figure 1.** Flowchart for transesterification.**Table 2. Fuel Characteristics**

| fuel | B0 | B8 | B16 | B24 | B100 | standard test method |
|---|--------|--------|--------|--------|--------|----------------------|
| lower heating value (kJ/kg) | 43,971 | 43,654 | 43,453 | 42,945 | 38,567 | ASTM D240 |
| density (kg/m ³ at 15 °C) | 830 | 842 | 847 | 853 | 887 | ASTM D1298 |
| kinematic viscosity at 30 °C (mm ² /s) | 3.2 | 3.3 | 3.5 | 3.7 | 4.6 | ASTM D445 |
| cetane number | 54 | 54 | 55 | 57 | 62 | ASTM D613 |
| fire point (°C) | 65 | 70 | 74 | 78 | 132 | ASTM D93 |
| acidity (mg KOH/g) | 0.057 | 0.062 | 0.072 | 0.094 | 0.279 | ASTM D664 |
| flash point (°C) | 60 | 66 | 94 | 102 | 124 | ASTM D93 |

**Figure 2.** Static immersion test of specimens exposed at different temperatures for 160 h.

ibility with elastomers at higher temperatures. Furthermore, the ratio of the agrofuel mixture may be changed for high-speed marine diesel engines according to the India Classification Society's recommendations on gasoline replacement for marine use. As a result, WCO is the most attractive alternate fuel attributed to its similar characteristics to diesel, and it is greatly lowering its reliance on crude oil.¹¹ Many investigations on several types of performance and emissions for the WCO have been extensively carried out in the past, and the details are provided in Table 1.

Contrarily, using biodiesel in compression ignition (CI) engines causes adversarial behavior with regard to material

Table 3. Specifications of the Universal Testing Machine

| | |
|----------------------|-------------|
| actuators capacity | 9 kN |
| stroke | ±28 mm |
| vertical day light | 565 mm |
| horizontal day light | 38 mm |
| rate of loading | 1.02 mm/min |

compatibility. There are four types of corrosion behaviors that apply to biodiesel: general, local, dry, and wet deterioration. Normal corrosion is a constant intrusion, while pitting is local corrosion brought on by ionic contaminants, acetic acid, and chloride ions. On the other hand, the polarity of the biodiesel

Table 4. Specifications of the Durometer

| | |
|---------------|----------|
| code | ISH-STAC |
| diameter | 100 mm |
| height | 75 mm |
| testing width | 65 mm |
| block weight | 1 kg |

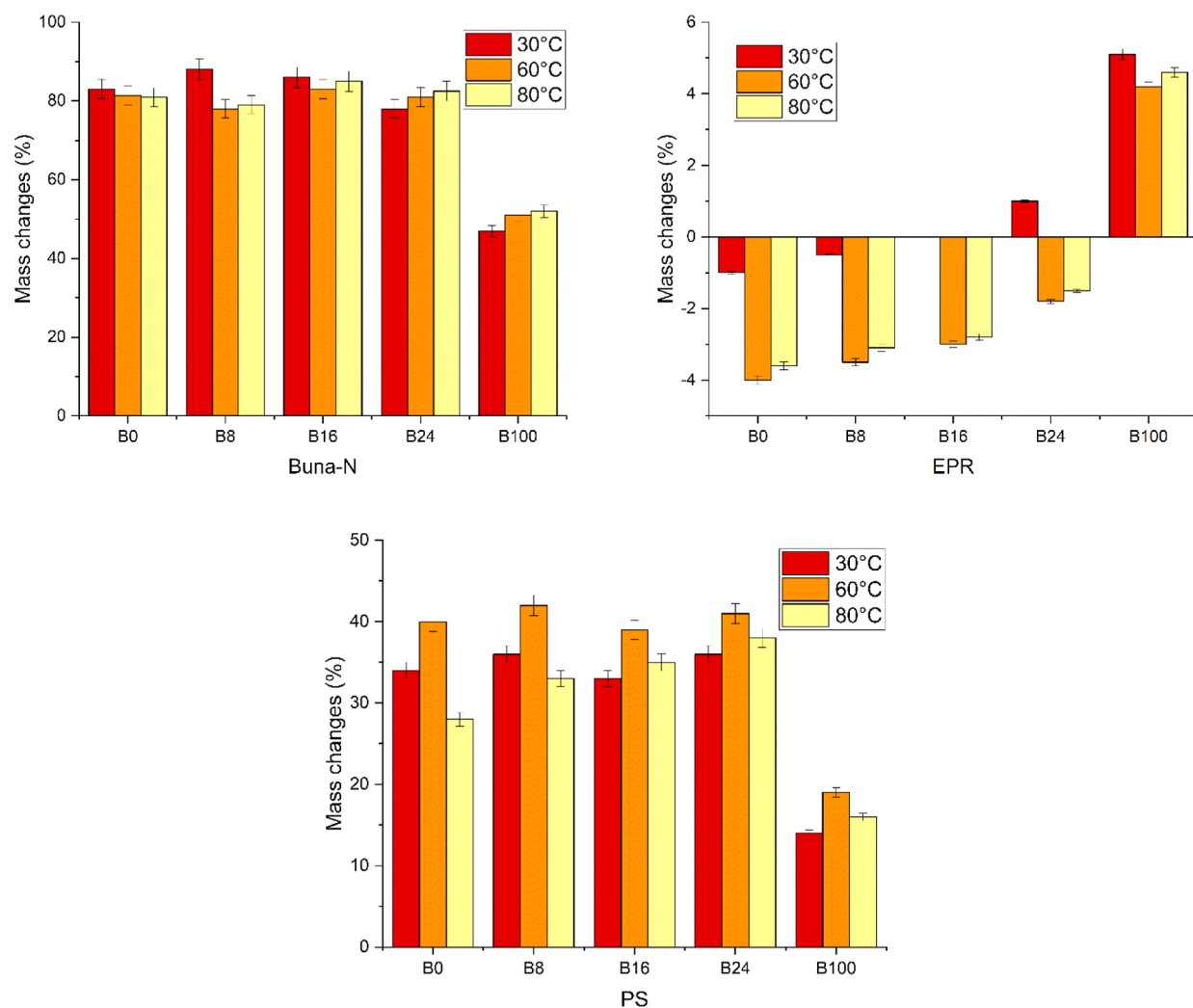
Table 5. Uncertainty Particulars

| parameters | accuracy | uncertainty percentage |
|------------------------------------|-------------|------------------------|
| mass (g) | ± 0.001 | ± 0.1 |
| volume (mm^3) | ± 0.01 | ± 0.4 |
| temperature ($^{\circ}\text{C}$) | ± 1 | ± 1.3 |
| force (N) | ± 0.1 | ± 0.5 |
| hardness (BHN) | ± 0.5 | ± 0.7 |

molecule is connected to dry corrosion. The bulk of the literature claims that using biodiesel in CI engines causes general and pitting corrosion that harm metallic parts. On metal surfaces, corrosion manifests as a series of holes. Although both types of corrosion may occur at the same time, pitting corrosion has a more detrimental impact. The main catalyst for the corrosion of metallic materials is the presence of certain organic acids, aldehydes, peroxides, ketones, and

esters in commercially available oxygenated fuels. Additionally, the presence of oxygen in the chemical makeup of fuels may contribute to the corrosion of metallic components of the engine and the fuel delivery system. As a result, because biodiesel is an oxygenated fuel, fuels that include it may induce corrosion on both metallic and nonmetallic surfaces. Biodiesel may degrade fuel tanks and pipelines because of its high solubility and hygroscopic, which can lead to corrosion residues or microbial activity. A small amount of acetic acid, which deteriorates steel when exposed to humidity, may be found in biodiesel. Also, the biodiesel water content can indicate the corrosive properties of the fuel.¹² As a result, the use of biodiesel causes uncommon problems, premature failure, and damage to the engine's internals. The question of the metal compatibility of biodiesel has therefore been the subject of several studies.

Ethylene propylene rubber (EPR)'s strong, saturated polymer backbone structure gives them exceptional resistance to heat, oxidation, ozone, and environmental aging. Both black and nonblack substances are appropriately pigmented. Two benefits include resilience to ozone and weather. They have a high level of resistance to chemicals and water. Their unsuitability for use as food and the presence of aromatic hydrogen are their drawbacks. EPR seals or pieces of sanitary

**Figure 3.** Graph depicting mass changes in rubber materials.

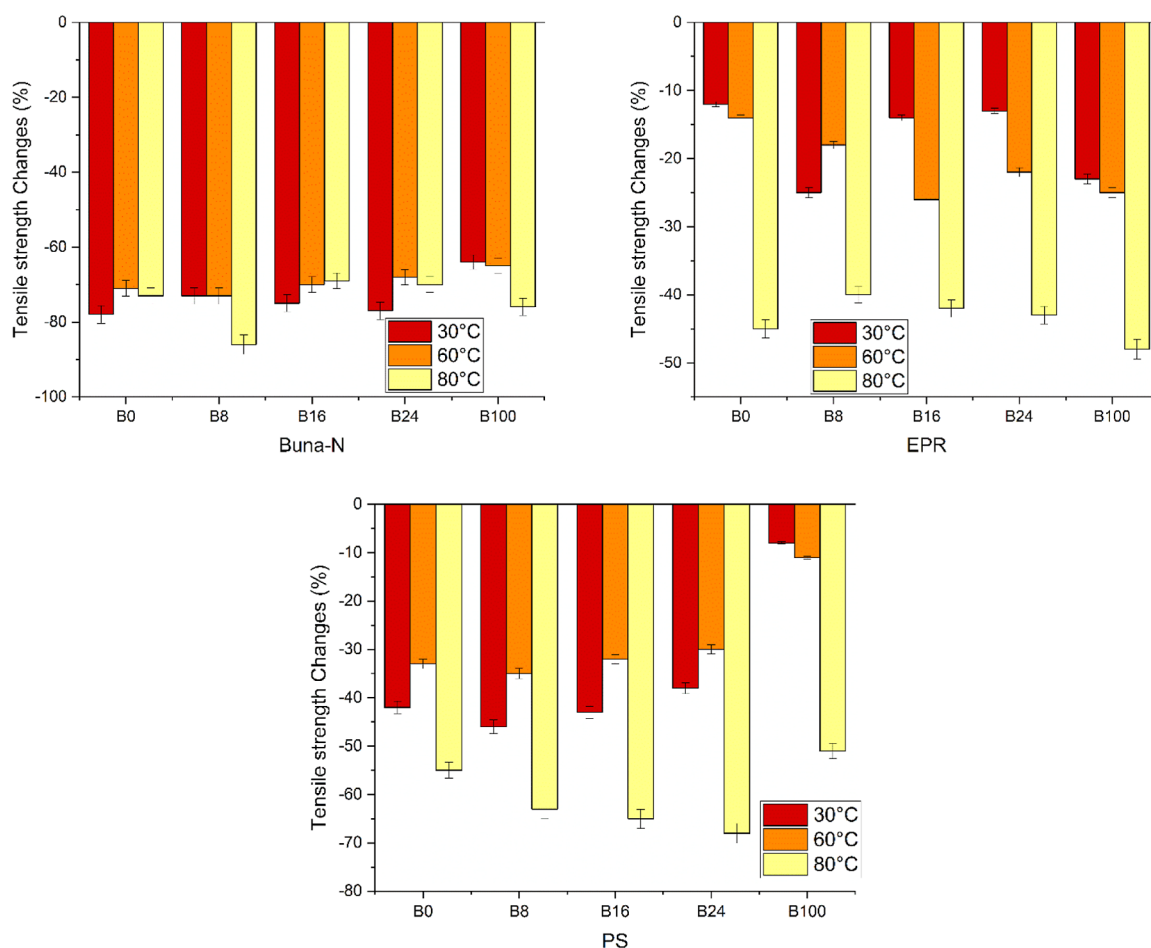


Figure 4. Graph depicting tensile strength changes of rubber materials.

equipment in a high-temperature water vapor atmosphere are reliable.¹³ In biofuel, many fatty acid alkyl esters are present. This leads to a series of problems, including gas seeping from the pipe and the pipe's seal cracking. The aforementioned problems are mostly brought on by aspects of the structure and molecular structure. Due to these characteristics, using agrofueled causes increased corrosion, which leads to the breakdown of turbine components.¹⁴ In addition, the agrofueled mixture exhibits considerable changes as a result of metal contacts with the turbine parts, particularly in terms of the total acid number, fuel viscosity, and thickness. In order to use agrofueled in a diesel turbine, research must be conducted to determine whether agrofueled and the elastomer raw materials of the turbine gasoline supply structure are compatible.¹⁵ It takes a lot of investigation and study to determine whether fuels used in turbine gasoline delivery techniques and single-feedstock agrofueleds such as canola oil and palm oil are compatible. All agrofueleds are regularly subjected to a consonance examination at a temperature of 25 °C.¹⁶ According to their dependence and motivating force, the obstacles are categorized by using the MICMAC study. The evaluations reveal that the primary barriers include subpar production facilities, inadequate processing technology, inconsistent supply levels, and problems with vehicle access.¹⁷ A study was conducted to determine the effects of agrofueled palm oil on the amount, harshness, and flexibility of various materials for use in CI engines. Some goods, such as ethylene-propylenediene monomer and chloroprene rubber, were shown to have

considerable differences in the aforementioned properties. Hansen solubility limits were used in a study to determine the commonality in the agrofueled mix using similar raisins. The findings revealed that the presence of aldehydic and short-chain acids leads to the deterioration of the agrofueleds, which in turn impacts their attraction for raisins. Additionally, it generates an extra bulge in materials including silicone, neoprene, fluorocarbon, and nitrile butadiene rubber (NBR), mostly because acetaldehyde is present.¹⁸ Additionally, the atomic structure of the raw material for agrofueled also had a greater influence on its compliance with agrofueled and NBR. The length of the carbon chain, the quantity of double bonds, and the chain length of the alcohol moiety of the fatty acid ester are additional factors that can influence the affinity of the agrofueled with the NBR. In addition, the original immersion method and the gasoline distribution method had been used to test the suitability of the rubber material with various fuel turbine operating settings.¹⁹ For these tests, biodiesel is made from spent cooking oil. When compared to base fuel, the B20 blend exhibits the shortest ignition delay, BTE, and smoke emission.¹⁰ Compared to the unique absorption method, the new technique could mimic real-world operating conditions for gasoline-powered turbines, particularly diesel-powered turbines that included variations in the turbine's temperature and gravity. These two play a crucial part in the research to determine the compatibility between agricultural fuel and the gasoline supply strategy used in a fully functional gasoline turbine.²⁰

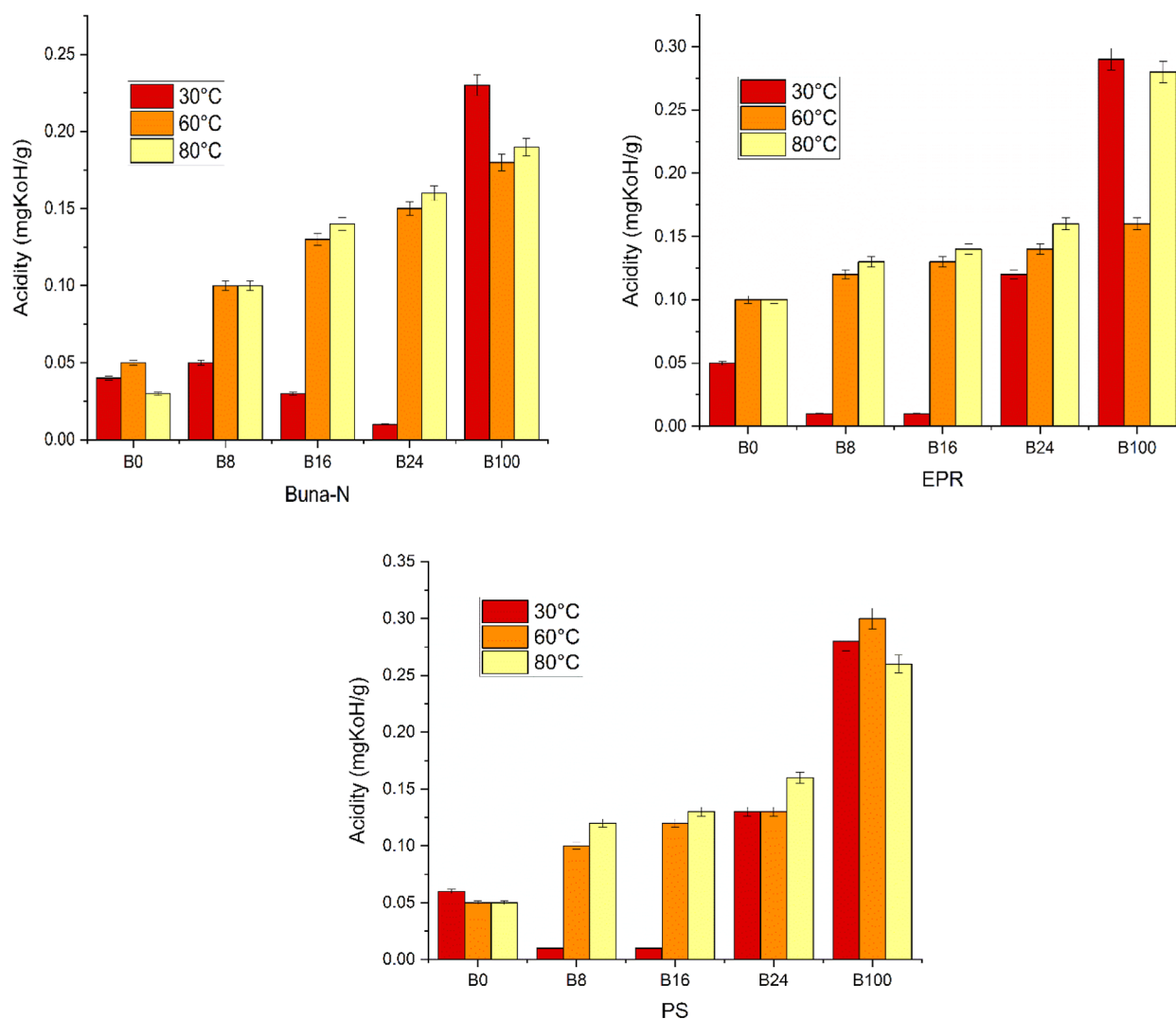


Figure 5. Graph depicting the acidity of rubber materials.

The temperature of the gasoline delivered to the container until the diesel is injected into the engine varies greatly depending on the mechanism used to distribute the diesel in gasoline turbines. Another study has focused primarily on agrofuel compatibility and the materials used in gasoline structure elastomers at various temperatures. The tenacity of nitrile rubber fuel valves between 30 and 65 °C was assessed using gravimetric measurements, tensile strength calculations, and scanning electron microscope examination.²¹ The findings revealed that while there is less loss of the NR fuel hose when the fuel temperature is adjusted and applied to the turbine, there is greater bulging when the amount of agricultural fuel blend and elastomers are reduced. The tensile strength of gasoline deteriorates when pipes are exposed to variable gasoline with a higher proportion of agricultural fuel. Using automotive polymeric materials comprising polyphthalamide and polyacrylamide, a study was done to determine the propensity of B0, B10, B20, and BD100 palm agrofuel mixes at 35, 65, and 85 °C. All polymeric materials showed a significant mass increase as the temperature rose.²² The palm oil biodiesel used for the experiment prepared two fuel blends B10 and B20. The nitrile rubber elastomer is mixed with the fuel. While increasing the biodiesel concentrations, density and viscosity are increased when compared with neat fuels. With higher

biodiesel mixes, the elastomer increased mass change by 58.1%, volume change by 58%, tensile strength by 53.5%, and hardness by 52% compared with base fuel.²³

At 25, 50, and 70 °C, the compatibility of B0, B10, B20, and BD100 palm biodiesel blends with automotive polymeric materials such as polyphthalamide and polyarylamide was examined. At higher temperatures, both polymeric materials showed a large mass increase.²⁴ The impact of biodiesel's molecular structure and feedstock on its compatibility with NBR was explored. It has been found that the fatty acid ester's carbon chain length, amount of double bonds, and alcohol moiety chain length all have a significant impact on its compatibility with the NBR.²⁵ A unique immersion approach was used to investigate the compatibility of biodiesel with fuel delivery system components under various diesel engine operating circumstances. In comparison to the traditional immersion method, the new methodology can simulate the real working conditions of diesel engines, including pressure and temperature variations, which are critical for estimating biodiesel compatibility with fuel delivery system materials under diesel engine working conditions.²⁶

Based on prior research, (i) the primary purpose of this study is to examine the impacts of ordinary fossil diesel and three distinct WCO biodiesels on diesel engine characteristics

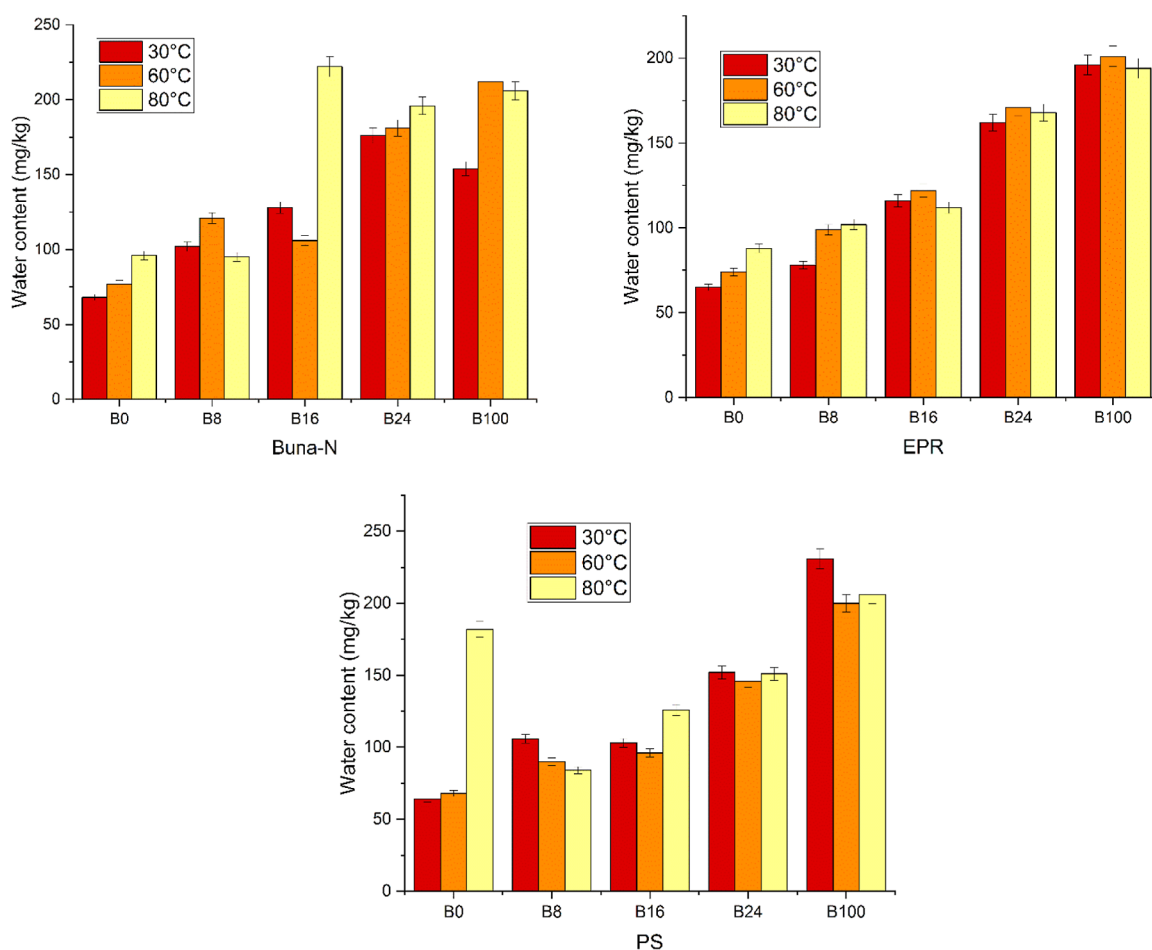


Figure 6. Graph depicting the water content of rubber materials.

and (ii) to comprehensively assess the compatibility of WCO biodiesel blends and elastomer parts in high-speed diesel engines; (iii) biodiesel blends (B8, B16, B24%, and pure WCO biodiesels) with Buna-N, EPR, and PS rubber were tested in a diesel engine at different temperatures of 30, 60, and 80 °C; and (iv) in addition to the immersion test, the acidic and moisture content of the WCO biodiesel and its blends were also evaluated.

PROCEDURE AND MATERIALS

The test WCO biodiesel fuels used in this investigation, designated B0, B8, B16, B24, and B100, were donated by Annamalai University in Tamil Nadu. The study primarily focuses on numerous process variables that are important in the production of biodiesel, particularly the influence of transesterification reaction variables on the properties of biodiesel. After the trans-esterification reaction, the esterified oil is put through a transesterification reactor to make biodiesel, which is then blended with methanol (12–18 wt %) and a base solution of solid KOH (0.58–0.74 wt %) in the esterified oil and heated for 0.6–1.2 h at 62–68 °C. After the transesterification procedure, the mixture is left to settle for 9–13 h in order to produce methyl ester. Figure 1 shows the flowchart for the transesterification process, and Table 2 shows the different fuel qualities of the tested WCO biodiesel and its blends.

Buna-N, EPR, and PS were among the most often utilized elastomer materials in the many components of high-speed

marine diesel engines, including fuel tanks, oil pipelines, fuel hoses, and seals. As a result, three elastomer materials that adhere to ASTM D471 were selected for this study: From each of the elastomer materials Buna-N, EPR, and PS, further square- and dumbbell-shaped samples are produced. The square-shaped sample was used to analyze the change in mass, volume, and hardness, while the dumbbell-shaped sample was used to analyze the change in tensile strength. Additionally, following processing, the fuel was transferred from the tank to the fuel injector via the fuel pump, filter, hose, and pipe. During this transfer, the temperature of the fuel should gradually rise. According to the temperature of the fuel in the tank, the high-pressure pipe, and the position of the fuel injectors, respectively, the actual temperature change in the fuel supply system was maintained at 30, 60, and 80 °C. Immersion experiments have been performed without the inclusion of liquid circulation, agitation, or disturbance of the corrosion system (Figure 2). The compatibility of three common elastomer materials, namely, Buna-N, EPR, and PS, with WCO biodiesel for use in high-speed marine engines has been examined in numerous investigations on static immersion at 30, 60, and 80 °C for 160 h. Before and after the immersion test, quantitative measurements of changes in physical attributes, primarily mass, volume, hardness, and tensile strength, were made. The mass fluctuations were measured using an analytical balance with a 5-decimal place in accordance with the ASTM D471 standard, and the volume variations were also measured.

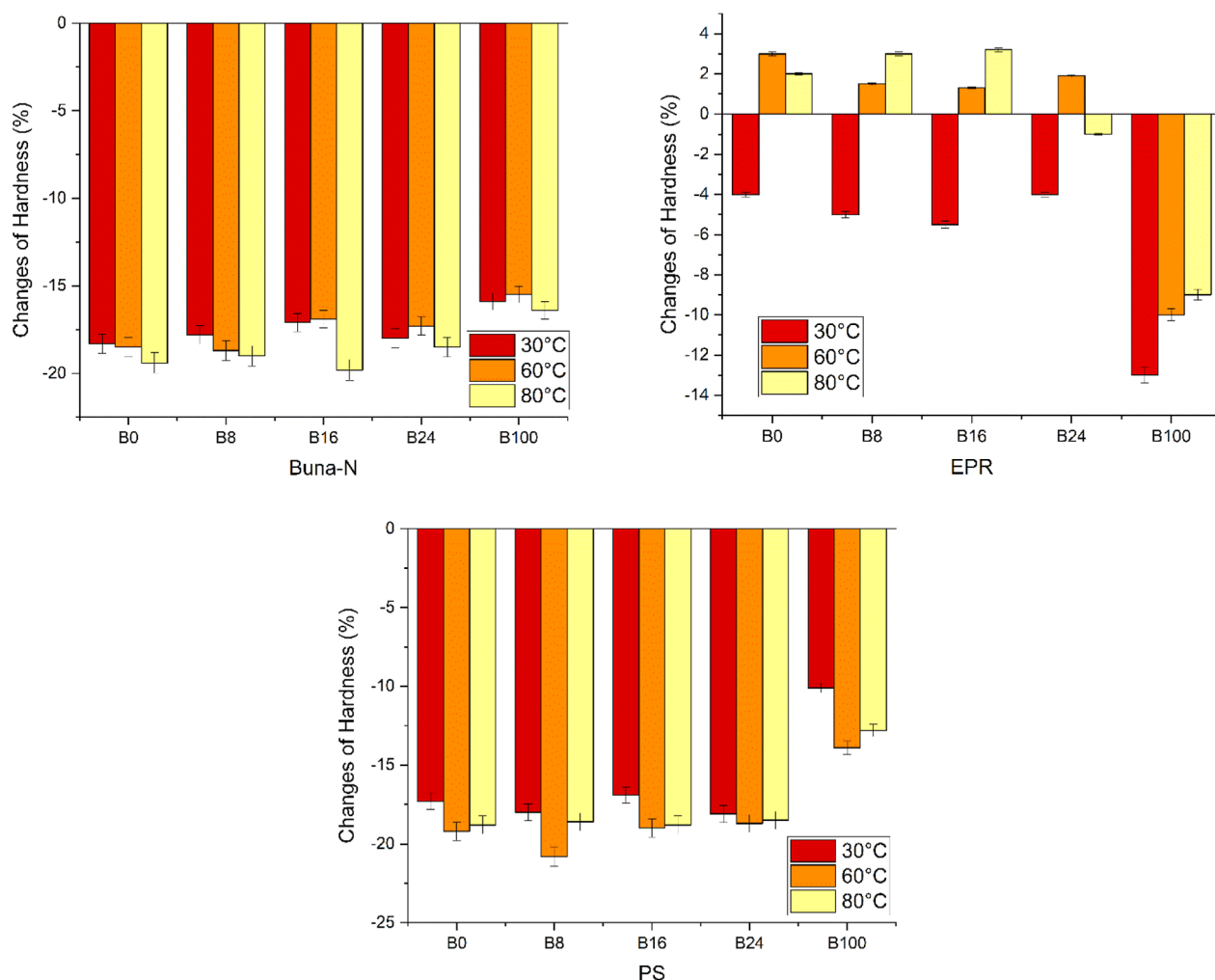


Figure 7. Graph depicting changes in the hardness of rubber materials.

Using ASTM D412-compliant dumbbell-shaped test samples with a gauge length of 30 mm, we determined the tensile strength on a DLD 2500 electronic universal testing machine. The hardness of the test samples was determined by using an ASTM D224-compliant durometer (model LX-A). The hardness of the test samples was determined using an ASTM D224-compliant durometer (model LX-A). Table 3 shows the specification of the universal testing machine, and Table 4 shows the specifications of the durometer.

Uncertainty Analysis. Uncertainty analysis was used to determine the experimental errors. The Gaussian-distribution method was used to assess the uncertainty of measured parameters using $+2\sigma$ confidence intervals. To calculate the uncertainty, measurements were made under similar operating conditions. Table 5 represents the uncertainty of the measurements used in the investigation.

The measured parameter's uncertainty is given by the formula $(\Delta X_i) = 2\sigma_i/\bar{x}_i \times 100$.

RESULTS AND DISCUSSION

Mass Changes. Figure 3 depicts the mass changes of three elastomer samples (Buna-N, EPR, and PS) after 160 h of exposure to different concentrations of a WCO agrofuel mix at temperatures of 30, 60, and 80 °C. It was observed that combining WCO with diesel or agrofuel and then pounding the mixture increased the mass of the elastomer materials.

Reducing the amount of WCO in the agrofuel mix below 24% resulted in a slight loss in mass. When less than 24% of the WCO agrofuel blend percentage was utilized, the mass of Buna-N and PS increased significantly on the application; however, the increase in B100 was significantly smaller.³² Buna-N, of the three elastomer products evaluated, expanded the most. Nonpolarity may decrease in nonpolar solvents due to the general rule that opposing components tend to evaporate in polar liquids.³³ Compared to 80 and 30 °C, a more significant mass change in Buna-N, EPR, and PS occurs at roughly 60 °C. An initial increase in rubber bulging occurs about 320 h after the first contact and then diminishes and stabilizes at room temperature. The peak of the bulging event is moved forward in time due to the fuel's temperature and the length of the flushing process. As a result, under standard diesel engine operating conditions, the bulging of engine parts can be controlled because of the bulging of the elastomer material at a high degree of engine heat.

Tensile Strength Changes. As can be seen in Figure 4, after 160 h of exposure to different WCO agrofuel combinations at 30, 60, and 80 °C, the tensile strength of the three elastomer substances examined increased significantly. When Buna-N and PS are exposed to WCO agrofuel, they have less tensile strength than EPR. Buna-N and PS lose less tensile strength and gain EPR as the volume of the mixture increases. Both EPR and PS were shown to lack ionic

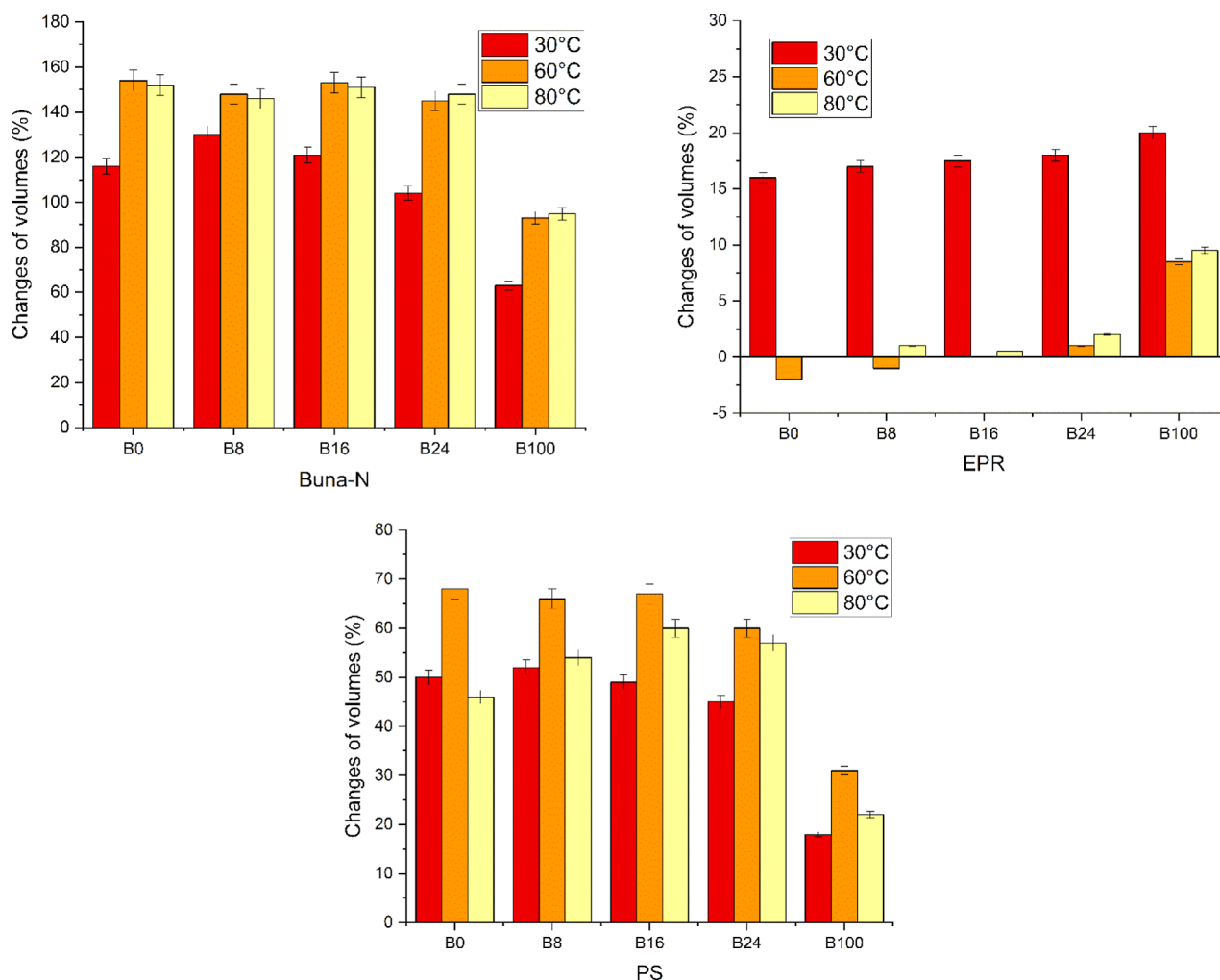


Figure 8. Graph depicts changes in the volume of rubber materials.

properties. Conversely, Buna-N is highly polarized. FAMES, an essential component of agrofuel, can be immersed without causing any friction owing to rubber's identical polarization level.³⁴ The observation of gas trapped within the elastomer substance chamber to maintain adequate inquiry into the impact of agrofuels on the elastomer structure. The correlation between the structure of the elastomer and the lower diffusion coefficient suggests that the lower diffusion coefficient may help to keep the protruding polystyrene (PS) bubbles in place. So that rubber can be used as an agrofuel for a long time, the right accelerator must be chosen.³⁵ Compared with interactions between polymers, interactions between solvents and polymers have a bigger effect on getting the material to bulge. Overall, an increase in the percentage of WCO in the agrofuel mix may not expedite the decrease in PS or Buna-N.

Acidity and Moisture Content. The components of the WCO agrofuel blend were tested for their acidity and moisture content. Figures 5 and 6 show the acidity and fluctuations in the moisture content of several WCO agrofuel blends exposed to Buna-N, EPR, and PS at 30 °C, respectively. Findings show that compared to diesel, B8, and B100, WCO agrofuel blends significantly decrease acidity and moisture levels after immersion. The conclusion is that the acidity of the agrofuel blend decreased following the Buna-N absorption trials; the drop must be a result of Buna-N expanding to its maximum extent after the experiment. In addition, the moisture content

of three elastomer compounds demonstrate a considerable decrease. Water immersion's effect on the elastomer's molecular structure might be significantly reduced compared to the moisture content.^{35–37} These numbers also show acidity and moisture content changes for various WCO agrofuel blends treated at 60 °C with Buna-N, EPR, and PS. After immersion, there is significantly less water, making it easier for the elastomer framework of the molecule to absorb water. During the research, the acidities of diesel, B8, B16, and B24 WCO agrofuel blends varied somewhat. However, the B100 acidity of gasoline remained significantly lower.^{36–39} As has been demonstrated, the elastomer can successfully absorb the agrofuel-free fatty acid component of WCO. In addition, these graphs illustrate the changes in acidity and water content of several WCO agrofuel combinations subjected to Buna-N, EPR, and PS at 80 °C. The diesel, B8, B16, and B24 WCO agrofuel blends exhibit minor changes in acidity, although the drop in the acidity of B100 is considerably smaller than that at 30 or 60 °C because a rise in temperature causes higher hydrolysis of FAMES.

Volume and Hardness Changes. As a result of the effect of agrofuel on the expansion of the elastomer, the solidity of the elastomer is diminished. Figures 7 and 8 demonstrate the quantity and solidity changes in three experimental elastomer substances during about 160 h of immersion in various experimental fuels at 30, 60, and 80 °C. Figures 7 and 8 show

that Buna-N and PS were immersed in diesel and WCO agrofuel mixtures; their volume increased, while their solidity decreased. According to studies, the quantity and density of Buna-N have changed, and the proportion of WCO in agrofuel blends has reduced to below 24%, with a significant decrease in B100. Buna-N had the most significant expansion in terms of quantity and density change. In addition, these results indicate that increasing the absorption at 60–80 °C does not reduce the frequency of volume and hardness changes. When this alteration was implemented, there was no significant difference in the volume adjustments of Buna-N and EPR between 60 and 80 °C. As depicted in Figures 6 and 7, the absorption of the molecular structure of the elastomer was commonly attributed to the cross-linking process, which is a significant factor in limiting the growth at a reasonable level.^{40–42} The reduction in the solidity of Buna-N and PS has been minimized by the increasing proportion of WCO agrofuel.

CONCLUSIONS

The purpose of this research is to explore the potential interactions between WCO biodiesel blends and elastomer materials such as Buna-N, EPR, and PS for usage in diesel engines at various temperatures. It also revealed the effect of the WCO biodiesel blending ratio on enhancing the absorption temperature of the elastomers. The following inferences can be drawn from this study;

- The use of elastomer materials like Buna-N, EPR, and PS in diesel engines is acceptable with WCO biodiesel blends.
- The outcome revealed remarkable behavior changes, including a minor increase in volume and a slight loss in tensile strength and hardness compared to that observed with neat diesel fuel.
- The expansion of rubber materials increases over 60 °C, although the rate of this process decreases above 80 °C.
- It has been found that the expansion of rubber materials is unaffected by the acid concentration of WCO biodiesel blends but significantly affected by the moisture content.
- WCO biodiesel's fundamental concepts are partly shaped by the WCO source and esterification process, which significantly impacts the fuel's attributes and features.

Future Recommendation

- Use of different types of biodiesel and rubber materials.
- Addition of nanoparticles into the fuels to see the behavior of the engine.

AUTHOR INFORMATION

Corresponding Authors

Elumalai Perumal Venkatesan – Department of Mechanical Engineering, Aditya Engineering College, Surampalem 533437, India; orcid.org/0000-0002-7536-8200; Email: elumalaimech89@gmail.com

Ravi Krishnaiah – School of Mechanical Engineering, VIT University, Vellore 632014, India; orcid.org/0000-0001-7911-0437; Email: ravikrish97@gmail.com

Emanoil Linul – Department of Mechanics and Strength of Materials, Politehnica University Timisoara, 300222 Timisoara, Romania; Email: emanoil.linul@upt.ro

Authors

Kalapala Prasad – Department of Mechanical Engineering, UCEK, JNTUK, Kakinada 533003, India

Sreenivasa Reddy Medapati – Department of Mechanical Engineering, Aditya Engineering College, Surampalem 533437, India

Sripada Rama Sree – Department of Computer Science Engineering, Aditya Engineering College, Surampalem 533437, India

Mohammad Asif – Department of Chemical Engineering, King Saud University, Riyadh 11421, Saudi Arabia

Sher Afghan Khan – Department of Mechanical Engineering, Faculty of Engineering, International Islamic University, Kuala Lumpur, Selangor 53100, Malaysia

Complete contact information is available at:

<https://pubs.acs.org/10.1021/acsomega.3c07871>

Notes

The authors declare no competing financial interest.

ACKNOWLEDGMENTS

The financial support from the Researchers Supporting Project (RSP2023R42), King Saud University, Riyadh, Saudi Arabia, is appreciated. The authors desire to show gratitude to the Mechanical Engineering, Aditya Engineering College, Surampalem, for the economic support extended in carrying out this research work.

REFERENCES

- (1) Parthasarathy, M.; Ramkumar, S.; Elumalai, P. V.; Kumar Gupta, S.; Krishnamoorthy, R.; Mohammed Iqbal, S.; Kumar Dash, S.; Silambarasan, R. Experimental investigation of strategies to enhance the homogeneous charge compression ignition engine characteristics powered by waste plastic oil. *Energy Convers. Manage.* **2021**, *236*, 114026.
- (2) Elumalai, P. V.; Parthasarathy, M.; Murugan, M.; Saravanan, A.; Sivakandhan, C. Effect of Cerium Oxide Nanoparticles to Improve the Combustion Characteristics of Palm Oil Nano Water Emulsion using Low Heat Rejection Engine. *Int. J. Green Energy* **2021**, *18*, 1482–1496.
- (3) Venu, H.; Raju, V. D.; Subramani, L.; Appavu, P. Experimental assessment on the regulated and unregulated emissions of DI diesel engine fuelled with Chlorella emersonii methyl ester (CEME). *Renewable Energy* **2020**, *151*, 88–102.
- (4) Elumalai, P. V.; Dhinesh, B.; Jayakar, J.; Nambiraj, M.; Hariharan, V. Effects of antioxidants to reduce the harmful pollutants from diesel engine using preheated palm oil-diesel blend. *J. Therm. Anal. Calorim.* **2022**, *147*, 2439–2453.
- (5) Elumalai, P. V.; Parthasarathy, M.; Hariharan, V.; Jayakar, J.; Mohammed Iqbal, S. Evaluation of water emulsion in biodiesel for engine performance and emission characteristics. *J. Therm. Anal. Calorim.* **2022**, *147*, 4285–4301.
- (6) Elumalai, P. V.; Annamalai, K.; Dhinesh, B. Effects of thermal barrier coating on the performance, combustion and emission of DI diesel engine powered by biofuel oil-water emulsion. *J. Therm. Anal. Calorim.* **2019**, *137*, 593–605.
- (7) Sivalingam, A.; Kandhasamy, A.; Senthil Kumar, A.; Perumal Venkatesan, E.; Subramani, L.; Ramalingam, K.; Thadhani, J. P. J.; Venu, H. Citrullus colocynthis—an experimental investigation with enzymatic lipase based methyl esterified biodiesel. *Heat Mass Transfer* **2019**, *55*, 3613–3631.
- (8) Praveena, V.; Martin, M. L. J. A review on various after treatment techniques to reduce NOx emissions in a CI engine. *J. Energy Inst.* **2018**, *91*, 704–720.

- (9) Atta, M.; Idris, A.; Bukhari, A.; Wahidin, S. Intensity of blue LED light: A potential stimulus for biomass and lipid content in fresh water microalgae *Chlorella vulgaris*. *Bioresour. Technol.* **2013**, *148*, 373–378.
- (10) Hu, Z. Y.; Luo, J.; Lu, Z. Y.; Wang, Z.; Tan, P. Q.; Lou, D. M. Interactions between Used Cooking Oil Biodiesel Blends and Elastomer Materials in the Diesel Engine. *ACS Omega* **2021**, *6*, 5046–5055.
- (11) Trakarnpruk, W.; Porntangjitlikit, S. Palm oil biodiesel synthesized with potassium loaded calcined hydrotalcite and effect of biodiesel blend on elastomer properties. *Renewable Energy* **2008**, *33*, 1558–1563.
- (12) Kumar, T. S.; Ashok, B. Corrosion behaviour analysis of SI engine components for ethanol-gasoline blends in flex fuel vehicular application. *Fuel Process. Technol.* **2023**, *240*, 107574.
- (13) Haseeb, A. S. M. A.; Jun, T. S.; Fazal, M. A.; Masjuki, H. H. Degradation of physical properties of different elastomers upon exposure to palm biodiesel. *Energy* **2011**, *36*, 1814–1819.
- (14) Megahed, M. M. Feasibility of nuclear power and desalination on El-Dabaa site. *Desalination* **2009**, *246*, 238–256.
- (15) Diez, L. I.; Cortés, C.; Pallarés, J. Numerical investigation of NO_x emissions from a tangentially-fired utility boiler under conventional and overfire air operation. *Fuel* **2008**, *87*, 1259–1269.
- (16) Mezher, N.; Rathbun, W. E.; Wang, H.; Ahmad, F. Chemical composition and screening-level environmental contamination risk of bioderived synthetic paraffinic kerosene (Bio-SPK) jet fuels. *Energy Fuels* **2013**, *27*, 3830–3837.
- (17) Xiong, Y.; Chen, G.; Guo, S.; Li, G. Lifetime prediction of NBR composite sheet in aviation kerosene by using nonlinear curve fitting of ATR-FTIR spectra. *J. Ind. Eng. Chem.* **2013**, *19*, 1611–1616.
- (18) Datta, R. N.; Huntink, N. M.; Datta, S.; Talma, A. G. Rubber Vulcanizates Degradation and Stabilization. *Rubber Chem. Technol.* **2007**, *80*, 436–480.
- (19) Mostafa, A.; Abouel-Kasem, A.; Bayoumi, M. R.; El-Sebaie, M. G. The influence of CB loading on thermal aging resistance of SBR and NBR rubber compounds under different aging temperature. *Mater. Des.* **2009**, *30*, 791–795.
- (20) Naik, S. N.; Goud, V. V.; Rout, P. K.; Dalai, A. K. Production of first and second generation biofuels: A comprehensive review. *Renewable Sustainable Energy Rev.* **2010**, *14*, 578–597.
- (21) Chai, A. B.; Andriyana, A.; Verron, E.; Johan, M. R. Mechanical characteristics of swollen elastomers under cyclic loading. *Mater. Des.* **2013**, *44*, 566–572.
- (22) Fröhlich, J.; Niedermeier, W.; Luginsland, H. D. The effect of filler-filler and filler-elastomer interaction on rubber reinforcement. *Composites, Part A* **2005**, *36*, 449–460.
- (23) Veza, I.; Zainuddin, Z.; Tamaldin, N.; Idris, M.; Irianto, I.; Fattah, I. R. Effect of palm oil biodiesel blends (B10 and B20) on physical and mechanical properties of nitrile rubber elastomer. *Results Eng.* **2022**, *16*, 100787.
- (24) Meenakshi, H. N.; Sah, A. P.; Sah, R. Deterioration of automotive polymeric materials in exposed to pongamia pinnata biodiesel. *Asian J. Chem.* **2017**, *29*, 1471–1476.
- (25) Zhu, L.; Cheung, C. S.; Zhang, W. G.; Huang, Z. Compatibility of different biodiesel composition with acrylonitrile butadiene rubber (NBR). *Fuel* **2015**, *158*, 288.
- (26) Chandran, D.; Ng, H. K.; Lik, H.; Lau, N.; Gan, S.; Choo, Y. M. Investigation of the effects of palm biodiesel dissolved oxygen and conductivity on metal corrosion and elastomer degradation under novel immersion method. *Appl. Therm. Eng.* **2016**, *104*, 294.
- (27) Nayak, S. K.; Hoang, A. T.; Nayak, B.; Mishra, P. C. Influence of fish oil and waste cooking oil as post mixed binary biodiesel blends on performance improvement and emission reduction in diesel engine. *Fuel* **2021**, *289*, 119948.
- (28) Lionus Leo, G.; Jayabal, R.; Srinivasan, D.; Chrispin Das, M.; Ganesh, M.; Gavaskar, T. Predicting the performance and emissions of an HCCI-DI engine powered by waste cooking oil biodiesel with Al₂O₃ and FeCl₃ nano additives and gasoline injection - A random forest machine learning approach. *Fuel* **2024**, *357*, 129914.
- (29) Ağbulut, Ü.; Yeşilyurt, M. K.; Sarıdemir, S. Wastes to energy: Improving the poor properties of waste tire pyrolysis oil with waste cooking oil methyl ester and waste fusel alcohol—A detailed assessment on the combustion, emission, and performance characteristics of a CI engine. *Energy* **2021**, *222*, 119942.
- (30) Gad, M. S.; Abu-Elyazeed, O. S.; Mohamed, M. A.; Hashim, A. M. Effect of oil blends derived from catalytic pyrolysis of waste cooking oil on diesel engine performance, emissions and combustion characteristics. *Energy* **2021**, *223*, 120019.
- (31) Ali S, S.; De Pours, M. V.; Damodharan, D.; Gopal, K.; Augustin, V. C.; Swaminathan, M. R. Prediction of emissions and performance of a diesel engine fueled with waste cooking oil and C8 oxygenate blends using response surface methodology. *J. Cleaner Prod.* **2022**, *371*, 133323.
- (32) Anil, P. M.; Patra, A.; Thangaraja, J.; Samuel, O. D.; Abbas, M. M. Assessment of Tribological Characteristics of Low-Sulfur and Ultralow-Sulfur Diesel under Practical Load and Temperature Scenarios. *SAE Int. J. Engines* **2021**, *15*, 15.
- (33) Kalam, M. A.; Masjuki, H. H. Testing palm biodiesel and NPAA additives to control NO_x and CO while improving efficiency in diesel engines. *Biomass Bioenergy* **2008**, *32*, 1116–1122.
- (34) Samuel, O. D.; Emovon, I.; Idubor, F. I.; Adekomaya, O. Characterization and Degradation of Viton Fuel Hose Exposed to Blended Diesel and Waste Cooking Oil Biodiesel. *J. Eng. Sci.* **2018**, *5*, G1–G8.
- (35) Kittur, M. I.; Andriyana, A.; Ang, B. C.; Ch'ng, S. Y.; Mujtaba, M. A. Swelling of rubber in blends of diesel and cottonseed oil biodiesel. *Polym. Test.* **2021**, *96*, 107116.
- (36) Kumar, S. S.; Rajan, K.; Mohanavel, V.; Ravichandran, M.; Rajendran, P.; Rashedi, A.; Sharma, A.; Khan, S. A.; Afzal, A. Combustion, Performance, and Emission Behaviors of Biodiesel Fueled Diesel Engine with the Impact of Alumina Nanoparticle as an Additive. *Sustainability* **2021**, *13*, 12103.
- (37) Aneeq, M.; Alshahrani, S.; Kareemullah, M.; Afzal, A.; Saleel, C. A.; Soudagar, M. E. M.; Hossain, N.; Subbiah, R.; Ahmed, M. H. The Combined Effect of Alcohols and Calophyllum Inophyllum Biodiesel Using Response Surface Methodology Optimization. *Sustainability* **2021**, *13*, 7345.
- (38) Ağbulut, Ü.; Sarıdemir, S.; Rajak, U.; Polat, F.; Afzal, A.; Verma, T. N. Effects of High-Dosage Copper Oxide Nanoparticles Addition in Diesel Fuel on Engine Characteristics. *Energy* **2021**, *229*, 120611.
- (39) Ağbulut, D. C.; Elibol, E.; Demirci, T.; Sarıdemir, S.; Gürel, A. E.; Rajak, U.; Afzal, A.; Verma, T. N. Synthesis of Graphene Oxide Nanoparticles and the Influences of Their Usage as Fuel Additives on CI Engine Behaviors. *Energy* **2022**, *244*, 122603.
- (40) Samuel, O. D.; Okwu, M. O.; Oyejide, O. J.; Taghinezhad, E.; Afzal, A.; Kaveh, M. Optimizing Biodiesel Production from Abundant Waste Oils through Empirical Method and Grey Wolf Optimizer. *Fuel* **2020**, *281*, 118701.
- (41) Verma, T. N.; Nashine, P.; Chaurasiya, P. K.; Rajak, U.; Afzal, A.; Kumar, S.; Singh, D. V.; Azad, A. K. The effect of ethanol-methanol-diesel-microalgae blends on performance, combustion and emissions of a direct injection diesel engine. *Sustain. Energy Technol. Assess.* **2020**, *42*, 100851.
- (42) Veza, I.; Deniz Karaoglan, A.; Ileri, E.; Afzal, A.; Tuan Hoang, A.; Tamaldin, N.; Gazali Herawan, S.; Abbas, M. M.; Farid Muhamad Said, M. Multi-Objective Optimization of Diesel Engine Performance and Emission Using Grasshopper Optimization Algorithm. *Fuel* **2022**, *323*, 124303.